Prospects for Higgs Searches at the TeVatron Run II

Arnaud Lucotte
on behalf of the CDF and DØ Collaborations

Institut des Sciences Nucléaire de Grenoble
53, av. des Martyrs, 38026 Grenoble Cedex
E-mail: lucotte@cern.ch

Although extensively sought this last decade, the Higgs boson still remains undetected. Relevant constraints on Higgs mass come from the direct searches performed at LEP, excludind Higgs with a mass lower than 114 GeV/c^2. The Fermilab TeVatron $p\bar{p}$ collider, with $\sqrt{s} = 2.0$ TeV will give the highest available center of mass energy until the LHC starts. Both CDF and DØ experiments are the only places where direct evidence of a Higgs signal can take place. This document reports the prospects for Higgs discovery at Run II, based on projections from the TeVatron Higgs Working Group analyses, and describe the progress made since then.

1 Introduction

The Standard Model (SM) of particle physics has been studied with very high precision over the past years and no significant deviations have been found. Still the particle that mediates electroweak symmetry breaking, the Higgs boson, remains undetected.
Run I Higgs searches at the TeVatron were luminosity limited, with a sensitivity to a standard Higgs production cross-section a factor 50 above that of the Standard Model prediction. The next run of the Tevatron offers reasons to be more optimistic. Based on a major upgrade of the accelerator chain, the design goal is to deliver about 15 fb^{-1} per experiment of $p\bar{p}$ collisions by the end of 2007. These performances represent a factor more than 100 enhancement with respect to Run I luminosity. CDF and DØ detectors have undergone major upgrades, both to adapt from increased collider performances and to improve significantely the physics reach based on new high performance tracking systems, and extended particle ID capabilities. Finally, all possible final states for Higgs searches have been analyzed, and have driven the developpement of specific triggers as well as software tools.

1.1 The Collider upgrade

The collider upgrade[1] is based on the replacement of the Main Ring, the last pre-acceleration stage originally used for the run I, by the Main Injector (MI). Located in a tunnel separate from that of the Tevatron, the MI is a new 120-150 GeV/c rapid proton synchrotron machine which improves significantly the $\bar{p}$-production capability.

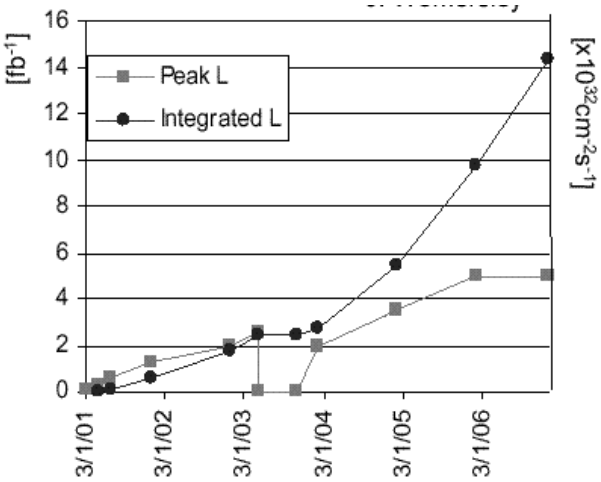

Figure 1: *TeVatron schedule from 2001 to 2007. The left axis indicates the integrated luminosity; Right hand axis reports instantaneous luminosity*

In the first period of Run IIa, the use of the MI coupled with upgrades in the $\bar{p}$-cooling and stacking [2], permits the use of more intense particule beams in the TeVatron. The number of circulating bunches is increased from 6×6 (Run I) to 36×36 in a first phase and eventually to 108×140, with a spacing between crossings respectively decreased from 4.2μs to 396 ns and eventually 132 ns in order to keep the number of interactions per crossing between 1-2. By that time, typical luminosity of 2×10^{32}cm^{-2}.s^{-1} will be reached, corresponding to a factor 10 enhancement in the delivered lumi-

nosity with respect to Run I performance by end 2003.
Run IIb is scheduled to start at the end of 2003 or 2004[3]. Improvements in the machine are expected from the use of the recycler ring as well as the use of a new cooling for the TeVatron beams. The Recycler ring[4], located in the same tunel as of the Main Injector, allows the re-use of those $\bar{p}$ remaining in the Tevatron at the end of a store, resulting in a factor 2 enhancement in the number of $\bar{p}$ available for collisions. It requires the use of a specific electron-beam cooling[5] adapted to high intensity $\bar{p}$ beams. At the same time, the TeVatron ring should benefit from the use of a new beam-beam conpensation system using high intensity electron-beam, designed to reduce beam emittance at the interaction points[6]. Combined, those upgrades are expected to achieve $5 \times 10^{32}\mathrm{cm}^{-2}.\mathrm{s}^{-1}$ in luminosity for an extra 13 fb^{-1} per experiment by the end of 2007. A preliminary schedule in term of luminosity is diplayed in Fig. 1.
Together with the luminosity upgrade, the increase in the beam energy from 0.9 TeV to 1.0 TeV allows a 40% enhancement in $t\bar{t}$ yields and a 20% increase in higgs production cross-section.

1.2 The Detectors upgrade

Both DØ and CDF detectors have undergone a major upgrade in preparation for the Run II. Detailed descriptions of the upgraded detectors may be found respectively in [7] and [8]. Both of them

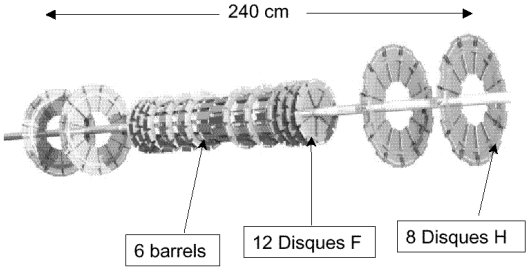

Figure 2: View of the New Tracking deveces in the D0 upgrade detector.

improved their capabilities in key fields for higgs searches: Track recontruction, momenta measurement, soft lepton triggering, secondary vertices tagging, displaced vertex triggering and jet energy resolution.

The new DØ Vertex detector is displayed in Fig 2. It is part of a new tracking system inside a 2T superconducting magnet and composed of a 4-layer Silicon Microstrip Traker for radii $\leq$ 10 cm, and of a 8-super-layer scintillating fibers device providing 16 measurements between 21 and 50 cm. A combined resolution of $\sigma_{\mathrm{p_T}}/\mathrm{p_T} = 0.2\%$ on momenta measurement is achieved over the range $|\eta| \leq 2.0$, while a 40 μm resolution in rϕ and 100 μm in rz on displaced vertices is expected. New scintillators-based pre-shower detectors have also been installed onto the calorimeter crystat walls and will help improve particle discrimination; the muon system benefits from an extension of the scintillators coverage both in the central and forward region, while the old forward muon chambers are replaced with fine granularity Mini Drift tubes extending up to $|\eta| \leq 2.0$. The calorimeter remains unchanged, except for a complete revision of its front end electronics. All electronic systems, DAQ and triggering architecture are also re-designed for run II.

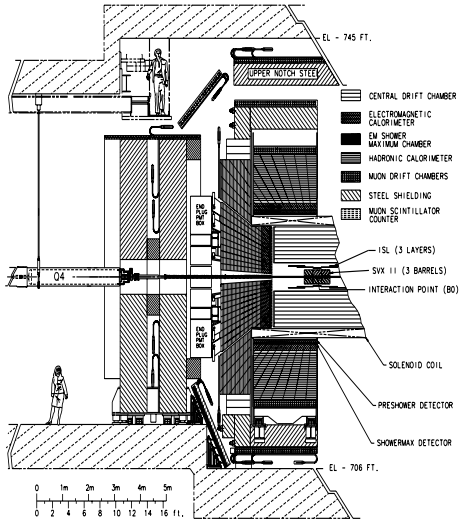

Figure 3: Longitudinal view of the CDF II detector

A view of the upgraded CDF II detector is displayed in Fig 3. The upgrade is based on the installation of an "integrated tracking system", combining a Silicon layer 0 around the beampipe with a 5-layer Vertex detector covering up to $|\eta| < 2$ at very small radii ($\leq$10cm), and two intermediate Silicon layers (at radii of 20-28 cm). This system provides $\mathrm{p_T}$ resolution better than 0.1%, high b-tagging efficiency and a stand-alone sili-

con tracking over the full region $|\eta| \leq 2.0$. A new Central Drift Chamber replaces the old Run I CTC, using small drift cells and fast gas to reduce drift times below 100 ns, will provide 96 measurements between 44 and 132 cm. The CDF II detector also includes an improved muon system, with new scintillators and fine granularity Muon Drift Chambers extending the present coverage in the forward region up to $|\eta| \leq 2.0$. Finally, while the scintillator-based central calorimeter remains unchanged for Run II, the gas calorimeter in the region $|\eta| \geq 1.0$ is replaced with a new scintillating tile plug calorimeter, with both new EM and hadron calorimeters.

2 Higgs Phenomenology

2.1 SM Higgs production and decays

The production cross-sections and decay branching ratios for Higgs boson are shown in Fig.7. The highest cross-section modes are $p\bar{p} \rightarrow H$ via gluon

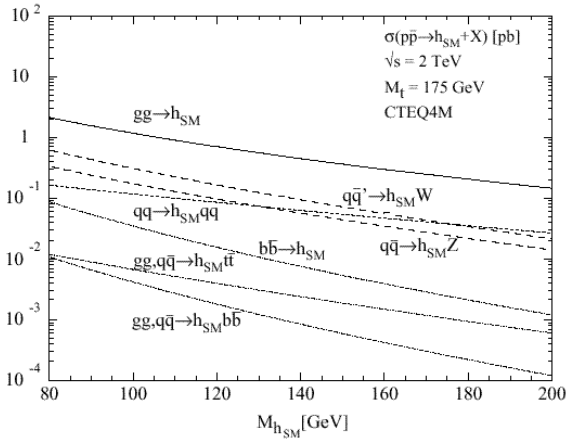

Figure 4: Standard Higgs production cross-section at $\sqrt{s} = 2.0\ TeV$

fusion, and the Higgs-strahlung processes $p\bar{p} \rightarrow HW$ and $p\bar{p} \rightarrow HZ$. The Higgs boson decays dominantely to the most massive kinematically allowed final state. That is $H \rightarrow b\bar{b}$ for $m_H < 135$ GeV with a Branching ratio of 80%, and $H \rightarrow WW^*$ for $m_H > 135$ GeV where one of the W may be off the mass shell. The lower mass analysis will thus seek final states with at least two b-jets. However QCD $b\bar{b}$ production with a cross-section of $100\mu b$ [9] make the $p\bar{p} \rightarrow H \rightarrow b\bar{b}$ mode impossible to exploit and leads to searches in $p\bar{p} \rightarrow W/ZH$ modes, where the boson is decaying into leptons.

2.2 Supersymmetric Higgs production and decays

Supersymmetric extensions of the SM give at least five physical Higgs states: two neutral scalars denoted h and H (with $m_h < m_H$), a single pseudoscalar A and a charge doublet $H^{\pm}$. At tree level, strong constraints apply to mass spectra that depend upon two parameters, chosen by convention to be m_A and $\tan\beta$ the ratio of the vacuum expectation values for the two higgs doublets. It is worthwile to note that, despite significant impact of the higher order corrections on the mass spectra, most SUSY models predict a lighter (neutral) Higgs with a mass below 130 GeV/c^2. For

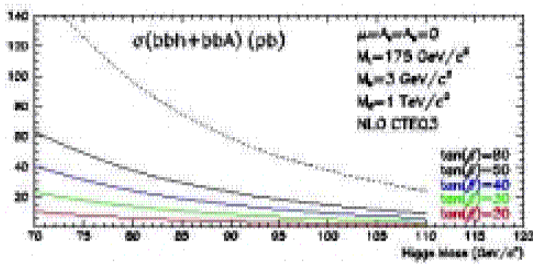

Figure 5: SUSY Higgs production cross-section for four b's final states Higgs

the lightest neutral higgs, MSSM phenomenology is similar to the SM. Production modes $p\bar{p} \rightarrow W/ZH$ have cross-sections that only differ by a factor $\sin^2(\beta-\alpha)$ wrt SM cross-sections. However, the gluon fusion mode $p\bar{p} \rightarrow h$ is enhanced by a factor $\tan^2\beta$. Higgs decay modes also differ from the SM modes since $hb\bar{b}, Ab\bar{b}$ and $Hb\bar{b}$ couplings are function of $\tan^2\beta$. As a results, the decay mode $h \rightarrow b\bar{b}$ is dominant over the full mass range $m_h < 200$ GeV and low mass SM Higgs searches can be easily converted to SUSY searches. Another consequence is that the four b's final state channel becomes significant, specially for high values of $\tan\beta$ as shown in Fig. 8. Charged higgs searches are made possible if $m_{H^{\pm}} < m_t - m_b$. In this case indeed, the Top quark decay mode $t \rightarrow H^+b$ can compete with the standard mode $t \rightarrow W^+b$ for both $\tan\beta \leq 1$ and $\tan\beta \gg 1$. Cross sections as function of Higgs mass is shown in Fig.9. In this mass range, charged higgs bosons decay dominantely to $H^+ \rightarrow \tau^+\nu$ (high $\tan\beta$) or

to $H^+ \to c\bar{s}, W^+ b\bar{b}$ (low tanβ).

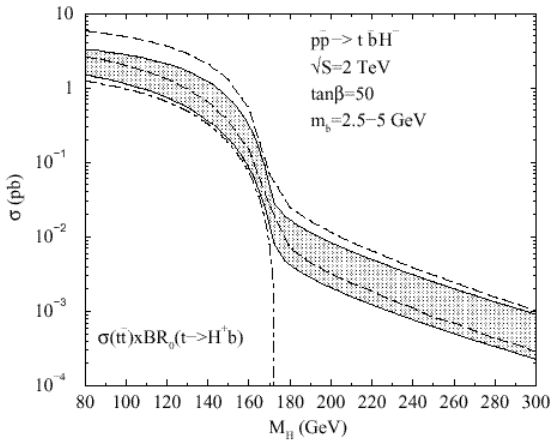

Figure 6: Top quark decay cross-section with one top decaying into a charged Higgs as function of $m_{H^\pm}$

3 Higgs Searches

All numbers quoted here are extracted from [10]. Generators used for signal and backgrounds are PYTHIA and ISAJET. Experimental efficiencies and background rejection are estimated with SHW[12], using parametrized resolutions for tracking and calorimeter systems to perform simple reconstruction of tracks, jets, vertices and trigger objects. DØ and CDF numbers. However, in all those specific issue detector specific full simulations have been performed to check those numbers.

3.1 Low Mass Higgs search ($m_H < 135$ GeV)

In the $110 < m_H < 135$ GeV/c^2 range, all possible final states have been investigated: $p\bar{p} \to WH \to l\nu b\bar{b}$, $p\bar{p} \to ZH \to \nu\bar{\nu}b\bar{b}$ and $p\bar{p} \to ZH \to l^+l^-b\bar{b}$. Common selections are based on the reconstruction of the b-quark invariant mass together with leptonic decays of the W/Z boson. Dominant backgrounds to these channels are $Wb\bar{b}$ and $Zb\bar{b}$ with b-quark pair from gluon radiation, single Top quark and top quark pair production. Key parameters for light mass Higgs searches are the following:

b-tagging: efficient b-tagging is mandatory to ensure the rejection of light quarks and c-quarks coming from standard backgrounds. Present studies based on full simulation indicate that more than 65% (single)-tag efficiency for less than 1% contamination are achievable for both DØ and CDF. This number includes displaced vertex tagging (typically more than about 50%) as well as soft leptons tagging (15% for both μ and e).

Mass reconstruction: Sensitivity to low mass higgs boson analysis depends strongly on the resolution achieved in the b-quark pair invariant mass. Improved mass resolution from 15% (typical Run I performance) to 9% resolution makes the signal significance increase by at least 1σ. This improvement can be made possible with the developpement algorithms taking into account charged track measurements in association with calorimeter-based jet energies. Although statistically limited in Run I, CDF already showed a 30% improvement in jet energy resolution[10] with respect to results not using such energy flow algorithms. Such performances still remain to be confirmed with new DØ studies.

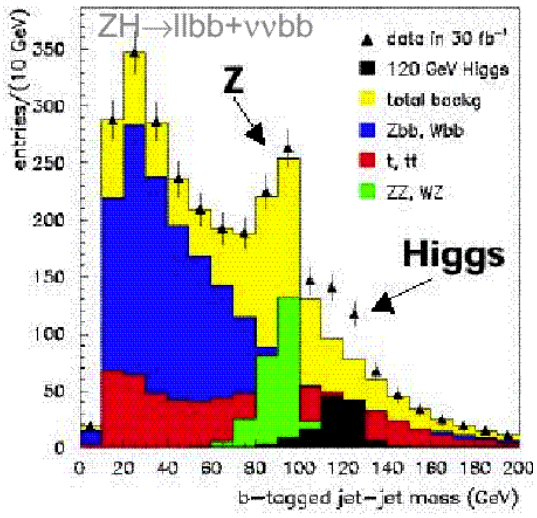

Figure 7: Invariant mass for a $m_H = 120$ *GeV* Higgs decaying into b-quark pair

$Z \to b\bar{b}$ **selection:** the selection of a large $Z \to b\bar{b}$ control sample is crucial for measuring b-tagging efficiency, demonstrating the ability to reconstruct $b\bar{b}$ resonances, optimizing mass resolution as well as for calibrating jet energy scale and measuring jet energy resolution. The selection will benefit from the developpement of specific triggers both in DØ and CDF all based on the detection of high p_T jets associated with two or more high

impact parameter tracks. Such algorithms have been implemented in Level 2 trigger systems, and preliminary results indicate that a yield of 25,000 $Z \to b\bar{b}$ events per fb^{-1} and per experiment could be reached.

Neural-Net (NN) techniques: additional multivariate analysis using Neural Network have also been applied. These techniques, used with success by DØ in the top quark mass and all-hadronic $t\bar{t}$ analyses, exploit topological differences in an optimal way and are shown to bring a factor 30% improvement with respect to classic cut-based analysis. The use of such techniques relies on a good MC simulation of signal and backgrounds (in both cross-section and shape), and thus necessitates progress in the full (NLO) calculations of $Wb\bar{b}$ and $Zb\bar{b}$ processes, which constitute the main backgrounds to low mass Higgs analyses.

		Higgs Mass (GeV/c^2)		
Channel	Rate	110	120	130
	S	1.9	1.2	1.8
$\nu\nu b\bar{b}$	B	8.0	6.5	4.8
	$S/\sqrt{B}$	0.7	0.5	0.3
	S	5.0	3.7	2.2
$l\nu b\bar{b}$	B	48	48	42
	$S/\sqrt{B}$	0.7	0.5	0.3
	S	0.8	0.5	0.3
$l^+l^-b\bar{b}$	B	2.5	1.8	1.1
	$S/\sqrt{B}$	0.5	0.4	0.3

Table 1: *Expected performance in terms of S and Background for 1 fb^{-1} luminosity*

Prospects for Run II have been established in [10] and are reported in Table 1 under the assumptions of a mass resolution of 9%, and b-tagging efficiency of 60%. Bringing back the mass resolution to 15% results in a degradation of about 0.1σ significance. Note that QCD $b\bar{b}$ background to the $p\bar{p} \to ZH \to \nu\bar{\nu}b\bar{b}$ channel is taken to be 50% of the total background and will be estimated using data. All three modes give similar sensitivity.

3.2 High mass Higgs searches

High mass range searches have used the following modes: $p\bar{p} \to H \to W^*W \to ll'\nu\nu$, $p\bar{p} \to WH \to WW^*W \to ll'3\nu$ and $p\bar{p} \to WH \to WW^*W \to ll'\nu\nu jj$. Common selection requires two high-p_T leptons with accompanying missing energy E_T^{mis}. Dominant backgrounds come from standard $p\bar{p} \to WW$, $p\bar{p} \to W$ + jets with fake leptons, $p\bar{p} \to t\bar{t}$ and $p\bar{p} \to \tau\tau$ productions. While 3rd jet veto and cut on the hadronic total energy help reject $t\bar{t}$ events, transverse mass $M_T(llE_T^{mis})$ is used against τ's.

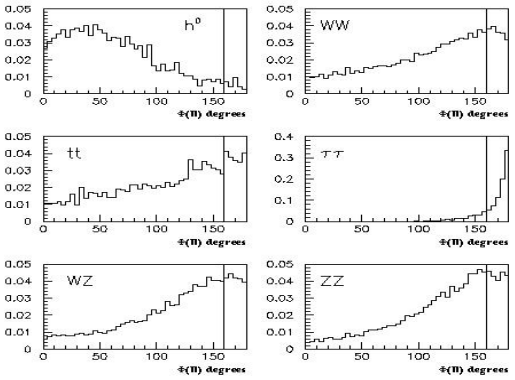

Figure 8: Spin correlation between leptons coming from W pairs in Higgs event compared to SM processes.

		Higgs Mass (GeV/c^2)		
Channel	Rate	140	160	180
	S	0.11	0.15	0.09
$l^\pm l^+ l^-$	B	0.73	0.73	0.73
	$S/\sqrt{B}$	0.13	0.18	0.11
	S	2.6	1.5	1.0
$l^+l^-\nu\bar{\nu}$	B	11	4.4	3.8
	$S/\sqrt{B}$	0.39	0.71	1.9
	S	0.34	0.45	0.29
l^+l^-jj	B	2.85	0.85	0.85
	$S/\sqrt{B}$	0.37	0.49	0.31

Table 2: *Expected performance in terms of S and Background for 1 fb^{-1} luminosity*

To disentangle between SM di-boson production and Higgs originated W's, spin correlations that exist between originated spin-0 bosons are extensively used in a discriminant function including $\Delta\Phi(l,l)$ (Fig.8) and $\Delta\theta(l,l)$. Finally the cluster mass $M_C = \sqrt{p_T(ll)^2 + M_T^2} + |\vec{E}_T^{mis}|$ is used to im-

prove standard background events rejection. Combining associate $p\bar{p} \rightarrow H \rightarrow WW^*$ with gluon fusion $p\bar{p} \rightarrow H \rightarrow WWW^*$ productions lead to about 2-3 expected events per fb^{-1} with $S/\sqrt{B} = 0.5 - 0.7$ in $150 - 160$ GeV/c^2 range. Sensitivity for different channels are reported in Table 2 [11].

3.3 *Neutral SUSY Higgs searches*

For lighstest mass Higgs results show that a 5σ discovery is possible with $20fb^{-1}$ per experiment for $1 < \tan\beta < 50$ and $80 < m_A < 400\ GeV$. For large values of $\tan\beta$ CDF searches for the modes $p\bar{p} \rightarrow \phi b\bar{b} \rightarrow b\bar{b}b\bar{b}$ with $\phi = h, H, A$ will seek final states with four b-jets, with at least 3 of them being tagged. All possible mass combinations of jets are computed and the distribution is compared with the expectations. 95% CL exclusion contour in the $\tan\beta$ vs m_A plane are shown in Fig.9.

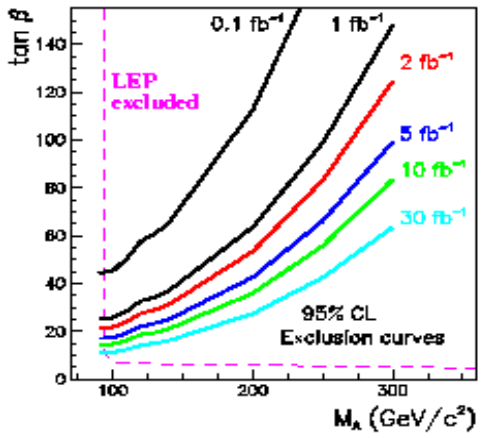

Figure 9: Neutral higgs exclusion contour in the $p\bar{p} \rightarrow h b\bar{b} \rightarrow b\bar{b}b\bar{b}$ channel for various luminosity hypotheses

3.4 *Charged Higgs searches*

Indirect searches is based on accurate determination of the $p\bar{p} \rightarrow t\bar{t}$ cross-section, where the Top quark decays into the SM mode $t \rightarrow W^+b$ with a Branching Ratio of nearly 1. Top quark selection criteria are well defined in [13]. Any deviation from the SM prediction can be interpreted as the occurrence of the competing SUSY mode $t \rightarrow H^+b$ with $H^+ \rightarrow c\bar{s}$ (low $\tan\beta$) or $H^+ \rightarrow \tau^+\bar{\nu}$ (high $\tan\beta$). Sensitivity to such events are luminosity-dependent. At Run II, about 1,000$t\bar{t}$ events per fb^{-1} are expected, making indirect searches more promising than direct searches until 2003. Projections are shown in Fig.10.

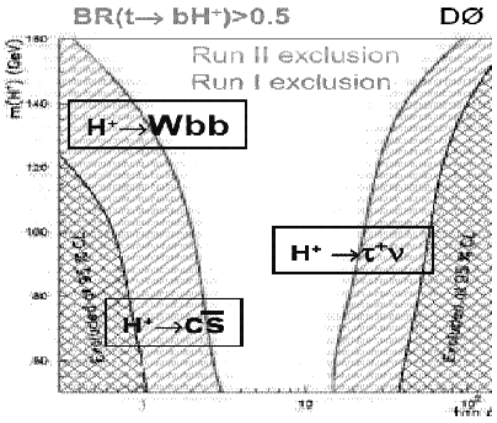

Figure 10: Charged Higgs reach at Run II from indirect searches

4 Conclusion

Run I searches were strongly luminosity limited. For Run II, the TeVatron Upgrade is expected to provide an integrated luminosity of $15fb^{-1}$ by the end of 2007. Together with the beam energy increase, this results in a factor 180 in the statistics available for Higgs study with respect to previous Run I performances. Both DØ and CDF detectors also have undergone major upgrades for Run II. New tracking devices have been installed in both experiments, including new high precision vertex detectors; Upgrades in muon and calorimeter detectors also leads to significant progress in lepton ID and coverage; Revisited triggering should allow the selection of $Z \rightarrow b\bar{b}$ high control samples mandatory to any low Higgs mass analysis. preliminary studies have quantified the importance of key sectors in Higgs searches, such as b-tagging, jet energy calibration and mass resolution. Analyses tools are continously being developped and should confirm the sensitivity of the TeVatron to exclude or discover Higgs with a mass below 180 GeV/c^2.

5 Acknowledgements

It is a pleasure to thank all the members of the DØ group at ISN Grenoble, Yannick Arnoud, Auguste Besson, Sabine Crepe, Pavel Demine and

Gerard Sajot for fruitful discussions over the last months. I would also like to thank John Womersley, Boaz Klima, John Hobbs, Ela Barberis and the members of the Higgs Working Group for their help in preparing the talk. A special thank to Elsa for her continuing support.

1. "Physics with the Main Injector", H.E. Montgomery, DPF99, UCLA, January '99, FERMILAB-Conf-99/057, hep-ex/9904019
2. "Pbar Upgrades for the TeVatron Collider", D.McGinnis,
   Beam Division seminar 5-23-00 see on page http://cosmo.fnal.gov/organizationalchart/mcginnis/Talks/Talks.htm
3. "Substantial Upgrades to the TeVatron Luminosity", M. Church, Moriond 2001
4. "Beams Division Preparation For RunIIb", D. McGinnis, PAC Apr 2001
5. "Prospectus for an Electron Cooling System for the Recycler", J.A. MacLachlan et al., Fermilab-TM-2061
6. "TeVatron Electron Lens Magnetic System", L. Tkachenko et al., PAC-2001
7. "The DØ detector at TeV33", the DØ collaboration, FERMILAB-PUB-98-095-E
8. "The CDF II Detector Technical Design Report", Fermilab-Pub-96/390-E
9. "Cross section for bjet production in pbapp collisions at 1.8TeV", Phys.Rev.Lett.85 5068(2000)
10. "Higgs Working Group Report", hep-ph/0010338
11. "Higgs boson discovery prospects at the TeVatron" P.Grannis & M.Rocco, World Scientific Apr 20,1999
12. SHW/PGS Documentation available from: http://www.physics.rutgers.edu/j̃conway/soft/shw/shw.html
13. Phys.Rev.Lett.83 1908(1999)